

PACS numbers: 87.63.– d; 87.64.Cc; 42.65.Re
DOI: 10.1070/QE2008v038n05ABEH013802

Study of the influence of glucose on diffuse reflection of ultrashort laser pulses from a medium simulating a biological tissue

A.V. Bykov, A.K. Indukaev, A.V. Priezzhev, R. Myllylä

***Abstract*. The influence of glucose on the diffuse reflection of near-IR femtosecond laser radiation from single- and three-layer media simulating biological tissues is studied experimentally. Based on a 800-nm femtosecond Ti : sapphire laser emitting 40-fs pulses and a VUV Agat streak camera, a setup is built for time and spatially resolved detection of radiation diffusely reflected from the volume of a strongly scattering medium. A multichannel fibreoptic system is developed for detecting pulses simultaneously at several fixed distances between a radiation source and detector. It is shown that the peak intensity and total energy of detected pulses are sensitive to variations in the glucose concentration in the medium under study from 0 to 1000 mg dL^{-1}. The relative sensitivity in our experiments achieved 0.030 % mg^{-1}dL.**

Keywords: *diffuse light scattering, ultrashort pulses, Ti:sapphire laser, streak camera, time-of-flight scheme, multilayer skin model, glucose detection.*

1. Introduction

One of the important problems of modern biomedical optics is the noninvasive measurement of the glucose concentration in blood and other human tissues. The solution of this problem will improve the quality of life of diabetics. In addition, the noninvasive method could provide a constant monitoring of the glucose level in the human blood [1]. This problem was investigated by many research groups by the methods of optical coherence tomography [2, 3], near-IR spectroscopy [4 – 6], and spatially resolved reflectometry [7, 8].

A.V. Bykov Department of Physics, M.V. Lomonosov Moscow State University, Vorob'evy gory, 119992 Moscow, Russia;
present address: Optoelectronics and Measurement Techniques Laboratory, University of Oulu, P.O. Box 4500, 90014 University of Oulu, Finland; e-mail: sasha5000@tut.by;
A.K. Indukaev, A.V. Priezzhev Department of Physics, M.V. Lomonosov Moscow State University, Vorob'evy gory, 119992 Moscow, Russia; e-mail: indukaev.a@gmail.com, avp2@mail.ru, avp2@phys.msu.ru;
R. Myllylä Optoelectronics and Measurement Techniques Laboratory, University of Oulu, P.O. Box 4500, 90014 University of Oulu, Finland; e-mail: risto.myllyla@ee.oulu.fi

Received 27 December 2007
Kvantovaya Elektronika **38** (5) 491 – 496 (2008)
Translated by M.N. Sapozhnikov

All the optical methods for measuring the glucose content by scattered radiation are based on the fact that variations in the glucose concentration in biological tissues or media simulating these tissues affect the scattering properties of these media. In particular, the scattering coefficient μ_s and anisotropy factor g strongly depend on the glucose concentration [5, 9]. The variations in these parameters are caused first of all by a change in the refractive index of the medium surrounding scatterers (skin cells or erythrocytes in blood), which in turn cause variations in the scattering cross section and phase function of scattering particles [10]. The influence of glucose on the scattering properties of a biological tissue and its models was experimentally estimated in papers [3, 9]. It was shown that a change in the glucose concentration by 1 mmol L^{-1} (18 mg dL^{-1}) reduced the scattering coefficient by 0.18 % – 0.22 %.

In our previous papers [8, 11 – 13], we studied numerically the possibility of detecting glucose in tissue models by the methods of spatially and time-resolved reflectometry by probing the media by ultrashort pulses. The aim of this paper is to study experimentally the influence of glucose on the diffuse reflection of femtosecond laser pulses from single- and three-layer media simulating biological tissues. We have shown that the probing of biological tissues by laser pulses of duration of a few tens or hundreds of femtoseconds is preferable than, for example, by picosecond pulses because it allows one to avoid the deconvolution procedure, which can introduce considerable distortions to the shape of the reconstructed pulses.

2. Experimental setup and objects

To study the influence of glucose on the diffuse reflection of ultrashort laser pulses from layered media, we developed a setup based on a femtosecond Ti : sapphire laser and a VUV Agat streak camera belonging to the Centre of collective use of the International Laser Centre, Moscow State University. The scheme of the setup is presented in Fig. 1. Femtosecond laser (*1*) emits 40-mJ, 800-nm, 40-fs pulses at a pulse repetition rate of 10 Hz. Laser radiation incident on beamsplitter (*2*) is divided into two beams. One beam is delivered through optical fibre (*6*) to the physical model (phantom) of biological tissue (*4*) under study and the other is delivered through an optical fibre directly to streak camera (*7*) and is used as a reference signal.

Note that laser radiation power was high enough and the required energy could be coupled into a fibre without focusing. The fibre end was located on the axis of the laser

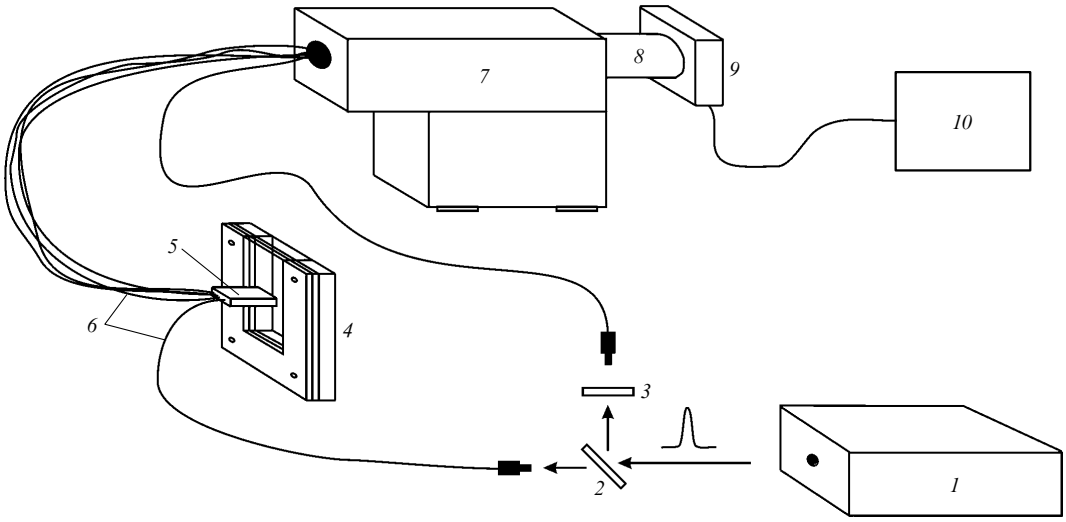

Figure 1. Scheme of the experimental setup: (*1*) femtosecond Ti : sapphire laser; (*2*) beamsplitter; (*3*) attenuator; (*4*) multilayer biological tissue model; (*5*) metal holder fixing the ends of optical fibres; (*6*) optical fibre; (*7*) streak camera; (*8*) imaging system; (*9*) CCD camera; (*10*) computer.

beam of diameter 1 cm. The saturation of the streak camera was avoided by placing attenuator (*3*) consisting of several neutral filters in front of the fibre transmitting the reference pulses. The duration of femtosecond pulses can increase during their propagation through neutral filters and the beamsplitter. However, this does not introduce considerable distortions to the results of measurements because this effect is much smaller than the pulse broadening in the fibre and the time resolution of the streak camera.

Radiation diffusely reflected from the phantom is collected by ten fibres in measuring head (*5*), which are located at different distances (from 530 μm to 5.3 mm) from the point of probe radiation coupling to the medium, and is delivered to the streak camera. The maximum time resolution of the streak camera used in our experiments was ~ 10 ps. The probe pulse was broadened after propagation through the light scattering medium and its duration at the input to the receiving fibre was several tens or hundreds of picoseconds depending on the source–detector separation.

Figure 2 shows the scheme of a fibreoptic measuring head for detecting radiation diffusely reflected from the object. It consists of eleven optical fibres enclosed in a metal holder of size 10×20 mm. The head was fabricated of ASF 300/330N fibres (Fiberguide Industries) in a protective nylon jacket with the numerical aperture NA = 0.22 and diameters 300/330/430/530 μm (core/cladding-1/cladding-2/buffer/jacket). The fibre of length 50 cm at the edge is used to couple probe radiation to the medium. The other ten fibres of length 75 cm are used to collect radiation diffusely reflected from the medium. The outputs of receiving fibres are enclosed in a metal holder, which is identical to that used to collect radiation and is fixed at the streak camera input. To detect correctly the shift of detected radiation with respect to probe radiation, an unscattered pulse is delivered to the streak camera through a fibre of length 125 cm. The lengths of fibres are chosen is such a way as to compensate the time delay of pulses propagated in them, i.e. the total fibre length of the fibre through which probe radiation is delivered and of transfer fibres is equal to the length of the fibre through which the reference pulse is delivered.

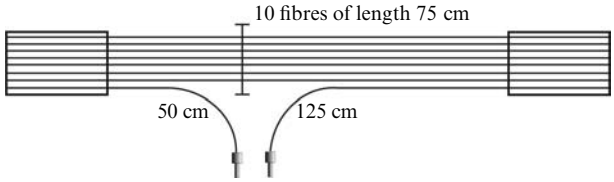

Figure 2. Scheme of a multichannel measuring head.

Radiation from the output of receiving fibres of the measuring head is delivered to the streak camera input (Fig. 3). The ends of fibres are imaged without magnification on the streak camera with the help of two identical objectives. The ends of fibres and the optical input of the streak camera are located in foci of the corresponding objectives.

Signals were detected and computer-processed with the help of an image sensing system based on a CCD camera (U2C-14C415 Ormins). By using a system of objectives, similar to that shown in Fig. 3, the image of the fluorescent screen of the streak camera was focused on the CCD matrix and then fed to a PC through the USB port.

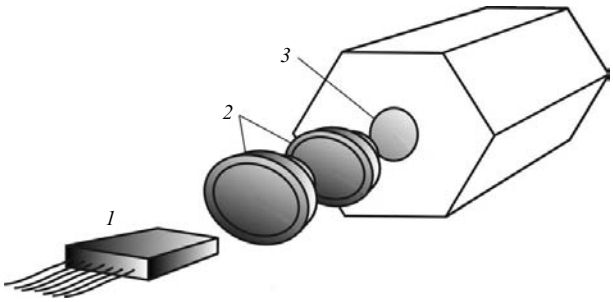

Figure 3. Scheme of the optical coupling of outputs of the measuring head to the optical input of a streak camera; (*1*) outputs of receiving fibres in a metal housing; (*2*) objectives; (*3*) optical input of the streak camera.

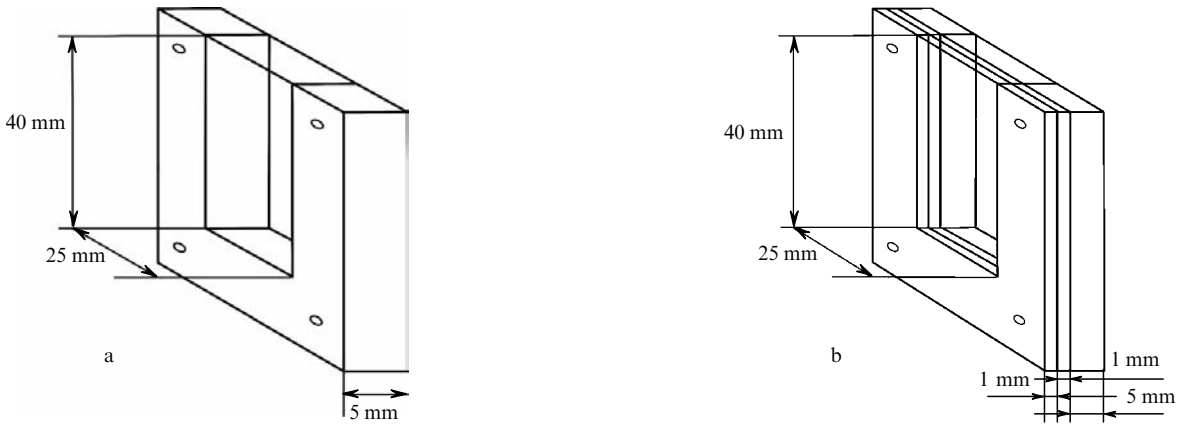

Figure 4. Design of cells for single- layer (a) and three-layer (b) models of biological tissues.

The optical contact of the measuring head with the medium (biological tissue phantom) is achieved by simple touching, without pressing, to avoid the deformation of the layered structure of the medium. The phantom was fabricated of a set of cells made of black plastic of different thicknesses, which were located one after another and fixed by screws, forming a multilayer medium. Each of the cells was filled with a certain light scattering liquid. The thickness of the medium layer in a cell depends on the wall thickness. The layers were divided by a 47 ± 1-μm-thick transparent adhesive (Scotch) tape. The refractive index of the Scotch tape measured with an optical coherence tomograph (Institute of Applied Physics, Nizhnii Novgorod; $\lambda = 910$ nm, resolution over depth 10 μm) was $n = 1.51 \pm 0.01$. We studied a 5-mm-thick single-layer phantom and a three-layer phantom with 1-mm-thick layers 1 and 2 and 5-mm-thick layer 3 (Fig. 4). The uniformity of the thickness of layers on the three-layer phantom was tested with the optical coherence tomograph.

Figure 5 shows the typical tomogram of an empty phantom (not filled with any liquid). Six boundaries corresponding to three dividing layers are distinctly observed. The far boundary is not seen because it is located outside the scanning range. We also tested the thickness of layers of the three-layer phantom filled with water to study the influence of liquids filling the phantom. Water was chosen as the filler in this case because the use of scattering liquids would not allow us to determine accurately the location depth of the walls. Diffuse scattering in the phantom was also measured by using other liquids (lipofundin-2% and blood with hematocrit 40 %); however, the thickness of the layers was the same as for water. Indeed, the thickness of layers 1 and 2 measured many times from tomograms in the empty and filled phantom was in the range from 900 to 1100 μm. Thus, the tomographic study of the phantom shows that the thickness of layers corresponds to the thickness of plastic cell walls within 10 %.

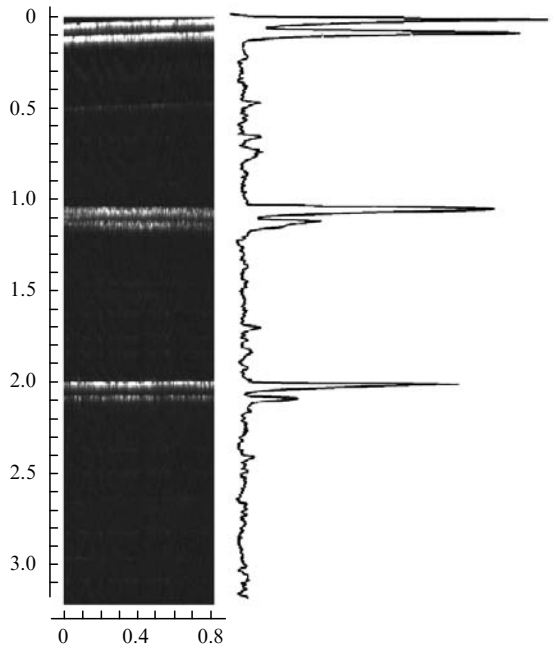

Figure 5. Typical tomogram of a three-layer cell without liquid (scale division is 0.1 mm).

3. Measurement procedure and results

We tested the single-layer phantom described above, which was filled with lipofundin (also called intralipid) at a concentration of 2 %. Lipofundin is a polydisperse suspension of spherical particles of radius ~ 0.3 μm in an aqueous solution with glycerol. The particles are droplets of soy oil covered with a 2.5 – 5-nm-thick lipid membrane [14, 15]. Lipofundin is completely biologically compatible and is used for parenteral nutrition of the sick. Lipofundin at different concentrations is used in physical models of biological tissues in biomedical optics. The optical properties of the aqueous solution of lipofundin at a concentration of 2 % in the near-IR spectral range are close to the optical properties of skin [16].

Figure 6 shows the typical image of the streak-camera screen obtained in our experiments on recording a pulse reflected from the phantom. The output signals of several first fibre detectors and the reference signal (on the right) are observed. The horizontal and vertical axes correspond to the spatial and time coordinates, respectively. The reference pulse is split into two pulses due to reflections from the two surfaces of the beamsplitter, the distance between the split pulses corresponding to the beamsplitter thickness in the time representation. The position of the reference pulse along the vertical on the screen is determined by the relation

between the distances from the beamsplitter to the entrance point of the pulse to the corresponding fibre and can be varied within the screen. One of the characteristic features of the streak camera is the presence of the so-called jitter, which is manifested in the displacements of successively recorded pulses on the screen along the time (vertical) axis with respect to their previous position by a random value. In our case, this random displacement achieved 100 ps. This is a serious problem in measurements with a high time resolution. However, the position of all the pulses on the horizontal axis is strictly fixed and is determined by the structure of the measuring head.

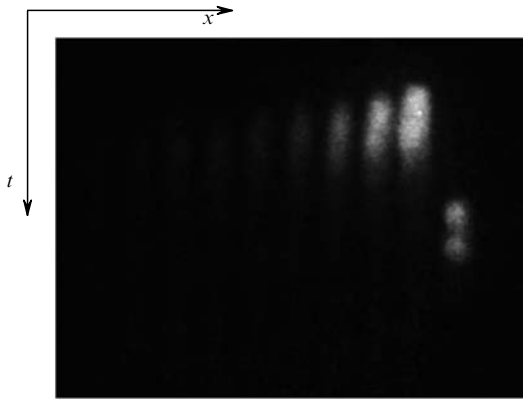

Figure 6. Typical image of the streak-camera screen obtained with a CCD camera recording a diffusely reflected pulse detected with a multichannel measuring head. The split in half image of the reference pulse is shown on the right.

To the left of the reference pulse (Fig. 6) the images of the output signals of successively located fibre detectors of the measuring head are observed. One can see that, as the distance from the source (not shown in Fig. 6) increases, the peak intensity of the reflected pulse, proportional to the illumination level, decreases, while the delay time with respect to the input pulse increases (the image of each successive signal is displaced along the time axis with respect to that of the previous pulse).

The measurements were performed in the following way. Several such images of the streak camera screen were recorded in the PC. The region along the x and t axes occupied by each signal was selected in each image, and spatiotemporal intensity distributions obtained in this way were averaged over several (as a rule, 25–30) pulses. Then, to exclude errors that could be caused by possible random jumps in the probe radiation intensity during experiments, pulse intensities obtained in this way were normalised to the reference pulse. The jitter was eliminated by displacing all the pulses along the time axis to make their leading edges coincident. Then, the corresponding pulses were averaged over all recorded images and the standard deviation was calculated.

Figure 7 shows the first part of the split reference pulse from which the time resolution of our system can be estimated (for example, by the pulse FWHM). This width is 13 ps in our case.

Consider a single-layer biological tissue phantom (Fig. 4a) filled with lipofundin-2 % with additions of glucoses at concentrations of 500 and 1000 mg dL^{-1} and

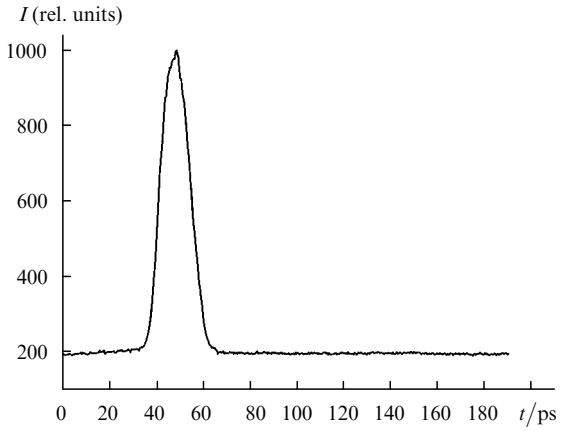

Figure 7. Signal intensity I reconstructed from the reference pulse image on the streak-camera screen.

without glucose. Recall that 500 mg dL^{-1} is the maximum admissible physiological concentration of glucose in the human blood, but to study the dependence of the parameters of detected pulses on the glucose concentration in more detail, we considered concentrations up to 1000 mg dL^{-1}. Figure 8 shows pulses from the first three fibres of the measuring head recorded for different glucose concentrations in the medium under study. One can see that the pulse intensity at the maximum decreases after the addition of glucose. This is explained by the fact that the addition of glucose reduces the scattering coefficient of the medium and increases the anisotropy factor [5, 9]. As a result, the higher the glucose concentration, the higher 'transparency' of the medium and the smaller the number of scattered photons returning to the rear half-plane and incident on detectors. Note that the intensity measurement error at the pulse maximum in Fig. 8 found experimentally was 15 %.

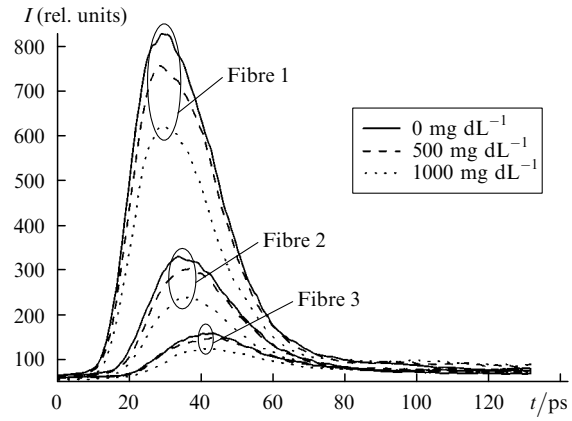

Figure 8. Intensities of backscattered pulses I detected in receiving fibres 1–3 of the measuring head at three glucose concentration.

Our Monte-Carlo calculations of scattered pulses [11–13] have shown that the most informative parameters of scattered pulses in the problem of glucose detection are their total energy (area) and peak intensity. Figure 9 presents the dependences of these parameters of the glucose concentration obtained in this paper.

The sensitivity of these parameters to the glucose content can be characterised by the slope of the straight lines in

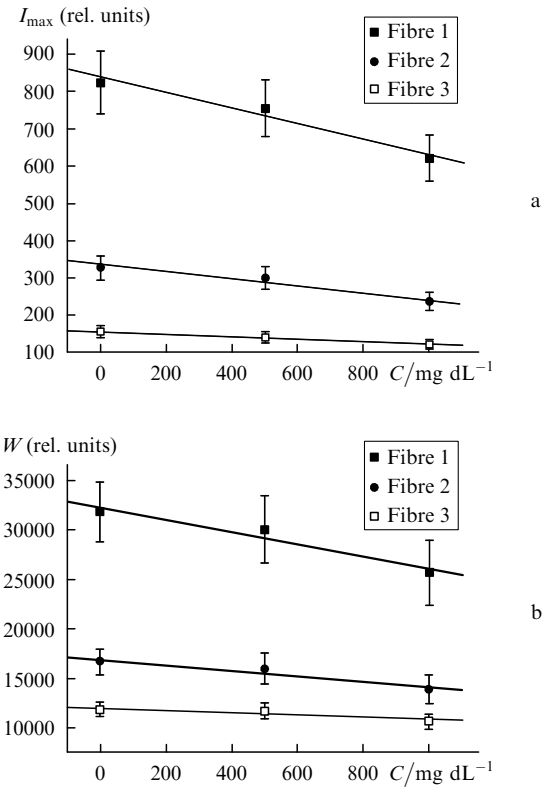

Figure 9. Dependences of the peak intensity I_{max} (a) and total energy W (b) of pulses detected in receiving fibres 1–3 of the measuring head on the glucose concentration C for the single-layer phantom.

Fig. 9. The larger is the slope, the stronger is the dependence of the parameter on the glucose concentration. One can see from Fig. 9 that the slope decreases with increasing the fibre number (i.e. with increasing the distance between the source and detector). The slopes for the peak pulse intensity are 0.20, 0.09, and 0.03 arb. units mg^{-1}dL for fibres 1, 2, and 3, respectively. For the total pulse energy, the slopes are 6.1, 2.7, and 1.2 arb. units mg^{-1} dL, respectively. To compare these parameters with each other, we introduce the relative sensitivity S_{value} to glucose defined as the relative change in the parameter per unit glucose concentration:

$$S_{value} = \left| \frac{value(0) - value(C)}{value(0)} \right| \frac{1}{C}, \qquad (1)$$

where value(0) and value(C) are the values of this parameter for the glucose concentration 0 and C mg dL^{-1}. The relative sensitivities determined by the peak pulse intensity S_I and the total pulse energy S_W calculated by expression (1) are presented in Table 1. One can see from this table that the peak intensity is more sensitive to variations in the glucose level.

Consider now a more realistic three-layer model of a biological tissue (Fig. 4b) in which layers 1 and 3 have thicknesses 1 and 5 mm, respectively, and are filled with lipofundin-2 % and glucose at concentrations 0, 250, and 500 mg dL^{-1}. Layer 2 of thickness 1 mm is filled with blood taken from the vein of a healthy volunteer. Before the experiment the whole blood was centrifuged for 3 min at the velocity 3000 revolutions per minute. The layer of white blood cells, thrombocytes, and plasma formed over red blood cells was removed and the obtained erythrocyte mass was diluted with a standard physiological solution and settled. This procedure was repeated twice to wash out erythrocytes carefully from the blood plasma and proteins contained in it, which cause aggregation. The obtained washed out erythrocyte mass was diluted with a physiological solution to a volume concentration of 40 %. This concentration (hematocrit) is typical of the blood vessels of humans. We prepared several samples of blood with added glucose at concentrations of 250 and 500 mg dL^{-1} and without glucose.

Table 1. Relative sensitivity of the peak intensity S_I and S_W to variations in the glucose level for the single-layer phantom and standard deviations from this level.

Detector number	S_I/% mg^{-1} dL	S_W/% mg^{-1} dL
1	0.025 ± 0.005	0.019 ± 0.005
2	0.027 ± 0.007	0.016 ± 0.004
3	0.022 ± 0.005	0.010 ± 0.003

The shape of pulses diffusely reflected from this medium is identical to the shape of pulses reflected from a single-layer medium and therefore is not presented here. Figure 10 shows the dependences of the peak pulse intensity and its total energy on the glucose concentration. One can see that, as in the case of the single-layer medium, the slope of straight lines decreases with increasing distance between the source and detector and, therefore, the absolute sensitivity determined by the slope decreases. However, as follows from Table 2, the relative sensitivity increases. In the case of the three-layer medium, the values of S_I and S_W for the corresponding detectors are close. Thus, in this case these parameters have the same sensitivity to variations in the glucose concentration.

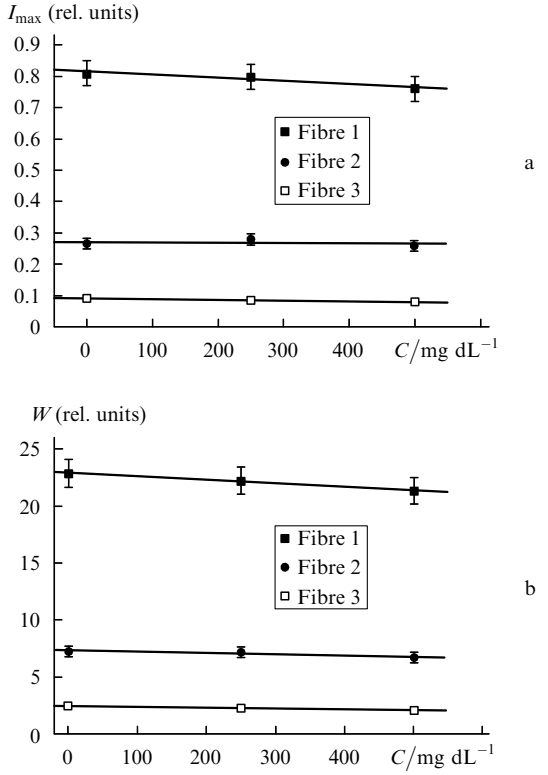

Figure 10. Dependences of the peak intensity I_{max} (a) and total energy W (b) of pulses detected in receiving fibres 1–3 of the measuring head on the glucose concentration C for the three-layer phantom.

Table 2. Relative sensitivity of the peak intensity S_I and S_W to variations in the glucose level for the three-layer phantom and standard deviations from this level.

Detector number	S_I/% mg^{-1} dL	S_W/% mg^{-1} dL
1	0.012 ± 0.003	0.013 ± 0.003
2	0.014 ± 0.004	0.015 ± 0.004
3	0.024 ± 0.006	0.030 ± 0.008

4. Conclusions

We have studied the influence of variations in the glucose concentration on the diffuse reflection of femtosecond pulses from single- and three-layer media simulating biological tissues. The earlier results of numerical simulations showing that the peak intensity of pulses and their total energy are sensitive to changes in the glucose concentration and can be used for its estimates have been confirmed. The relative sensitivity of these parameters has been experimentally found for different source–detector separations. For the single-layer model, the most sensitive parameter is the peak pulse intensity. For the first fibre detector (separated by 0.53 mm from the source), the sensitivity is 0.025 % mg^{-1} dL^{-1}, for the second fibre (separated by 1.06 mm from the source) – 0.027 % mg^{-1} dL^{-1} and for the third detector (separated by 1.59 mm from the source) – 0.022 % mg^{-1} dL^{-1}. For the three-layer model, these parameters have almost the same relative sensitivity. In particular, for the peak pulse intensity in the first, second, and third detectors, the sensitivity is 0.012, 0.014, and 0.024 % mg^{-1} dL^{-1}, respectively.

Acknowledgements. This work was supported by the Russian Foundation for Basic Research (Grant No. 06002-17015-a) and GETA Graduate School and Infotech Oulu (Finland). The study was performed by using the equipment of the Center of collective use of the International Laser Center, Moscow State University. The authors thank A.B. Savel'ev-Trofimov, R.V. Volkov, and D.A. Uryupina for technical assistance and consultations.

References

1. McNichols R.J., Cote G.L. *J. Biomed. Opt.*, **5**, 5 (2000).
2. Kuranov R.V., Sapozhnikova V.V., Prough D.S., Cicenaite I., Esenaliev R.O. *Phys. Med. Biol.*, **51**, 3885 (2006).
3. Larin K.V., Motamedi M., Ashitkov T.V., Esenaliev R.O. *Phys. Med. Biol.*, **48**, 1371 (2003).
4. Yamakoshi K., Yamakoshi Y. *J. Biomed. Opt.*, **11** (5), 054028 (2006).
5. Tarumi M., Shimada M., Murakami T., Tamura M., Shimada M., Arimoto H., Yamada Y. *Phys. Med. Biol.*, **48**, 2373 (2003).
6. Maruo, K., Tsurugi M., Chin J., Ota T., Arimoto H., Yamada Y., Tamura M., Ishii M., Ozaki Y. *IEEE J. Sel. Top. Quantum Electron.*, **9** (2), 322 (2003).
7. Bruulsema J.T., Hayward J.E., Farrell T.J., Patterson M.S., Heinemann L., Berger M., Koschinsky T., Sandahl-Christiansen J., Orskov H., Essenpreis M., Schmelzeisen-Redeker G., Boecker D. *Opt. Lett.*, **22**, 190 (1997).
8. Bykov A.V., Kirillin M.Yu., Priezzhev A.V., Myllula R. *Kvantovaya Elektron.*, **36**, 1125 (2006) [*Quantum Electron.*, **36**, 1125 (2006)].
9. Kohl M., Essenpreis M., Cope M. *Phys. Med. Biol.*, **40**, 1267 (1995).
10. Tuchin V.V. *Optical Clearing of Tissues and Blood* (Bellingham, Wash.: SPIE Press, 2006).
11. Popov A.P., Priezzhev A.V., Myllylä R. *Kvantovaya Elektron.*, **35**, 1075 (2005) [*Quantum Electron.*, **35**, 1075 (2005)].
12. Kirillin M.Yu., Bykov A.V., Priezzhev A.V., Myllylä R. *Proc. SPIE Int. Soc. Opt. Eng.*, **6445**, 64450U (2007).
13. Kirillin M.Yu., Bykov A.V., Priezzhev A.V., Myllylä R. *Kvantovaya Elektron.*, **38**, 486 (2008) [*Quantum Electron.*, **38**, 486 (2008)].
14. Flock S.T., Jacques S.L., Wilson B.C., Star W.M., van Gemert M.J.C. *Lasers in Surgery and Medicine*, **12**, 510 (1992).
15. Van Staveren H.G., Moes C.J.M., van Marle J., Prahl S.A., van Gemert M.J.C. *Appl. Opt.*, **30**, 4507 (1991).
16. Troy T.L., Thennadil S.N. *J. Biomed. Opt.*, **6**, 167 (2001).